OPEN ACCESS

Saudi Journal of Civil Engineering
Abbreviated Key Title: Saudi J Civ Eng
ISSN 2523-2657 (Print) | ISSN 2523-2231 (Online)
Scholars Middle East Publishers, Dubai, United Arab Emirates
Journal homepage: https://saudijournals.com/journal/sjce/home

Original Research Article

An Integrated Approach for Structural Crack Monitoring: Combining Plastic Tell Tales and Image Analysis for Enhanced Structural Health Evaluation

Adnan[1*], Ahmad Jawad[1], Hassam Raza[1], Dawood Shah Alam[1]

[1]BE Civil, Department of Civil Engineering, Sarhad University of Science and Information Technology

DOI: https://doi.org/10.36348/sjce.2024.v08i09.001 | **Received:** 29.09.2024 | **Accepted:** 04.11.2024 | **Published:** 07.11.2024

***Corresponding author:** Adnan
BE Civil, Department of Civil Engineering, Sarhad University of Science and Information Technology

Abstract

Structural Health Monitoring (SHM) calls for the development of the ideas of safety and main ability of civil structures. The most critical of the aspects explored in the paper is the safety monitoring of the structural configuration of any civil engineering work. Supervision of any sign of an odd shift from the usual state of structure enables one to prevent and or counter severe loss. It also depends on other environmental parameters such as load, nature of a seasonal parameter and the type of soil. Within this research project the Al-Beruni Academic Block of Sarhad University of Science and Information Technology is taken to monitor the cracks using Glass Tell-Tales, to collect data on cracks of buildings and during seismic activity, observe, study the cracks that are present.

Keywords: Structural Health Monitoring, Crack Detection, Plastic Tell Tales, ImageJ, Digital Image Processing, Structural Integrity.

1. INTRODUCTION

Structural integrity plays a vital role in safeguarding the building safety and duration; in areas where seismic activity is more common, [1, 2]. Structural Health Monitoring (SHM) systems serve as a key tool for judging and surveillance of structures offering timely information about possible degeneration or failure [3, 4]. According to this, the Al-Beruni block at Sarhad University of Science and Technology, constructed between 2014 and 2015, has shown cracks which require need to be assessed immediately [5, 6]. The cracks which develop in these systems are an early indicator of potential structural problems and are critical for evaluating the building's ability to sustain environmental stresses, especially seismic events [7, 8]. Maintaining the structural integrity and long term safety of structural components relies on the detection and analysis of cracks [9, 10]. Buildings, particularly schools, are vulnerable, both physically and institutionally, to cracks [11, 12]. The fact that these cracks are present in the Al-Beruni block as a whole presents cause for concern with regard to its structural durability, particularly in stress from seismic activity [13]. In one case, SHM applications for composite materials such as fiber reinforced and biocomposites were explored by Hamdan and Mustapha (2019) who showed that SHM systems can be used to measure stress and strain in the materials [14]. Past studies demonstrating unanticipated catastrophic failure when other forms of deterioration went undetected and undetected are highlighted as examples of the importance of failing to catch structural deterioration early on so that such catastrophes are averted [15, 16]. Together with others in the field, their work points to the need for systematic investigation of health of civil structures in areas of known seismic risk [17]. This research was motivated by the need for enhanced methods to monitor cracks that can contribute unique crack behavior information under different environmental and seismic loadings [18]. Traditional monitoring methods have limited precision for accurate evaluation of these complex structures, such as educational buildings [19]. This study bridges existing gaps in literature by focusing on effects of environmental factors and seismic events on the structural integrity by analyzing the Al-Beruni block. The practical implications of this study will be significant for the engineers, architects and policymakers working in the design, monitoring and maintenance of educational infrastructure in seismically active regions [21, 22]. The significance of this work goes beyond the Al Beruni block, the aim being to expand this research for advancing of crack identification and assessment techniques in the field of SHM [23]. Consequently, structures must now be able to not only withstanding daily operational stresses, but must also be resilient in the unavoidable presence of natural disasters in the face of increasing frequency of seismic events everywhere in the world [24]. Related to this, Van Steen and Verstrynge (2021) explored degradation monitoring in reinforced concrete structures showing it could use monitoring techniques to monitor for corrosion related cracking, thus highlighting the need for advanced crack monitoring strategies [25, 26]. The insights from this research will be used to inform the enhancement of existing safety protocols and to inform future design practice specifically of educational infrastructure in seismically active areas [27]. The overall aim of this work is based upon a complete examination of the cracks on the Al-Beruni block including patterns, sizes and locations which should determine the state of structural integrity of the building currently [28]. The importance of this analysis is to understand the performance of the building in similar future environments as well as for its forecasting for performance during future seismic events [29]. The research will further explore the correlations between seismic loads and crack propagation by analyzing data on how crack behavior reacts to seismic activity [30]. According to Charbonnel (2021), suggested the application of advanced modal analysis techniques to assess structures for which the loads are dynamic, similarly, the objectives of this research [31, 32].

In this study the use of modern SHM techniques, such as digital image correlation (DIC) and strain gauging, will increase the accuracy and reliability of the assessments that are made. Bogusz *et al*., (2022) demonstrated that digital image correlation is effective to map strain on structural elements and materials [33, 34]. The research integrates these advanced technologies in order to revise traditional crack evaluation methods for a more precise and actioned oriented insight regarding the life of the Al Beruni block [35]. The quality of the findings will be enhanced, and valuable tools for future monitoring of similar structures will be available [36].

Broader implications for the safety and maintenance of educational infrastructure in earthquake prone areas are expected from this research [37]. In areas where natural disasters are common such as earthquake, whilst ensuring the safety of students and staff in education buildings is a critical concern [38]. The results of this study will provide a basis for the assessment of the structural health and develop the effective maintenance strategy that should influence the future design and monitoring practices for educational institutions in similar geological context [39, 40].

Additionally, this research attempts to increase the knowledge on how seismic action degrades the structural integrity of educational structures [41]. Drawing together findings from previous work, and using new data collected using advanced SHM techniques, this study will provide a comprehensive view of theoretical and practical issues. With the inclusion of more advanced monitoring techniques such as the digital image correlation, the shortcomings of traditional methods including visual inspections and the use of physical gauges will be covered [43, 44].

In this research, we introduce a novel approach, called “Plastic Tell Tales and ImageJ”, to combine our more effective crack assessment monitoring methods [45]. Simple plastic tell tales are used to give visual indication of fracture movement, imageJ is used to image and analyze visual data more in detail [46]. The combination of these techniques enables a higher level of facility monitoring that provides precursory data for early detection of structural problems [47]. These tools for the integration are then able to have continuous monitoring of cracks, and understand their behaviour and progression under several ecological and seismic conditions [48].

Finally, this research of the Al-Beruni block structural integrity will enhance the understanding of how crack behaves in buildings in connection to the seismic activity [49]. Advanced SHM techniques will be utilized in the form of digital image correlation, the novel “Plastic Tell Tales and ImageJ” method, to increase the precision and reliability of crack monitoring [50]. Similarly, this study will not only provide solutions to the unique challenges of Al Beruni block but also provide helpful guidance towards making educational buildings safer and easier to maintain in seismic prone areas [51, 52].

2. METHODOLOGY

2.1 Plastic Tell Tales

Simple mechanical devices for monitoring movement over cracks are known as plastic tell tales [53]. They consist of two overlapping plates: Both were calibrated with millimeter markings and one with a transparent cursor. The Relative position of the plates is shifted by any movement, in which the plates are fixed on opposite sides of the crack. It allows for direct visual measurement of the crack’s expansion or contraction to a resolution of 1 mm which is largely why plastic tell tales (PA) are widely used in civil engineering to assess preliminary cracks and ongoing monitoring [54].

2.2 ImageJ Software

With ImageJ, an open source software image processing program, the power tools for analyzing crack images with precision are available [55]. Users can perform geometric transformations, measure pixel intensities, and estimate crack dimensions (size, length, width, and angle), among others, on the software. The main advantage of ImageJ is its ability to analyze images at different scales to extract this information, even as small changes in crack progression [56]. Supplementing the data gathered from plastic tell tales, ImageJ was used here to provide extremely detailed measurements of crack geometry.

2.3 Plates

A tell-tale is a part which comprises two flat cards in contact with one another along a half-length of one side. One is in mill metric scale one is transparent glass with hair line cursor in it. For a given load and crack width the one plate is lengthened while the other is shortened or vice versa.

2.4 Relation of the Cursor:

The position of the cursor in relation to scale indicates what amount of movement takes place. Range ± 20mm – Resolution 1 mm.

2.5 Model:

The standard Tell-Tale which is made of durable acrylic plastic is for measuring displacement across the cracks in the vertical and horizontal planes on flat surfaces, of the total volume expansion coefficient, 7 x 10 -5 cm/cm/C is thermal expansion coefficient.

2.6 Visual Rapid Screening of Al-Beruni Block

Rapid Visual Screening (RVS) is an approach for very fast evaluation of building sensitivity through visual inspection [57]. When a structure is identified as possibly seismic, it should be further evaluated by a planning professional knowledgeable in seismic planning to determine that the structure is really not Earthquake resistant. The methodology of the RVS procedure depends on a survey of a building sidewalk and a data collection form that the surveyor completes after making a visual observation outside the building and (if possible) from inside [58]. But if the number of buildings is large, doing a building RVS can reduce the number of buildings that need a detailed evaluation. For all buildings except cable structures, a rapid visual screening is useful [59]. Such an implementation of the RVS method allows for the relatively quick and inexpensive generation of a list of possibly dangerous buildings without the high expense of making a detailed seismic analysis of each individual building. The updated version of FEMA’s rapid visual inspection of buildings for potential seismic hazards is available. The RVS is conducted primarily for purposes of assessing seismic hazards such that building owners are informed of the need to reinforce or reinforce (where applicable) their buildings as well as allied hazards associated with the existing building. retroactive measures. RVS scores can use buildings to be identified. The vulnerability assessment by a numerical rating system of each building can be used as a prioritization tool [60].

2.7 Plan of Al - Beruni Block:

Figure 1: Al-Beruni Block

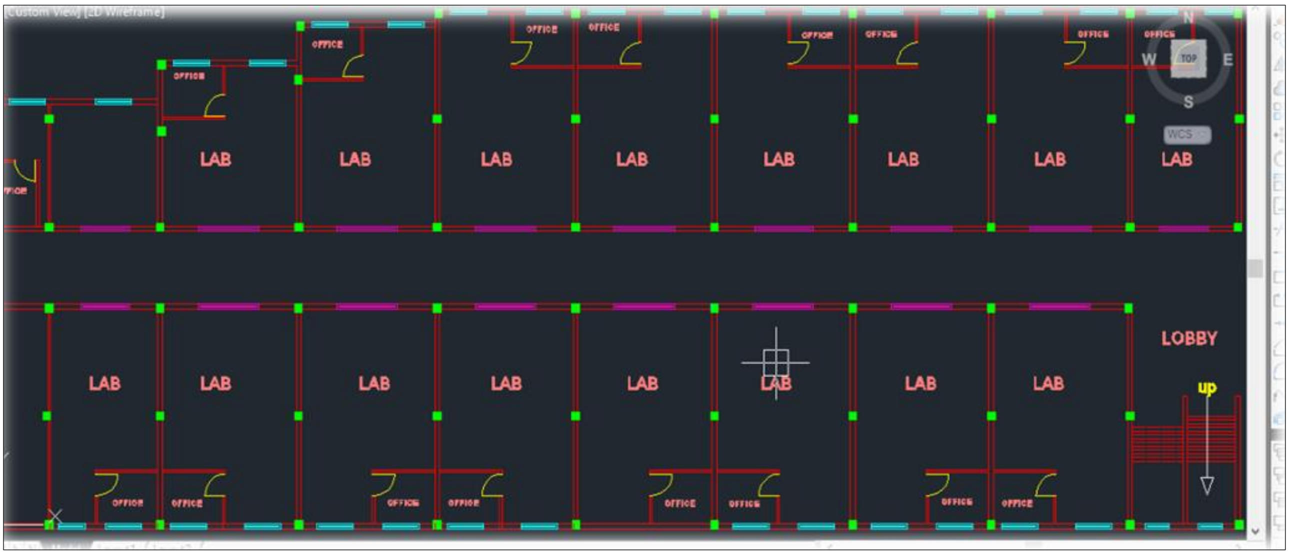

Fig. 2: Basement plan

The structural layout of the foundation in the Al-Beruni Block is shown in the basement plan. This figure shows in detail the key structural elements, the load bearing walls, columns and the support beams that make up the foundation base of the building. But understanding this plan is important because it helps to evaluate how cracks in the foundation can disrupt the entire stability of the structure. Ground conditions and soil movements go directly into the basement's structural integrity that supports the upper levels. If we see any cracks, those cracks are likely early signs of a larger, structural problem.

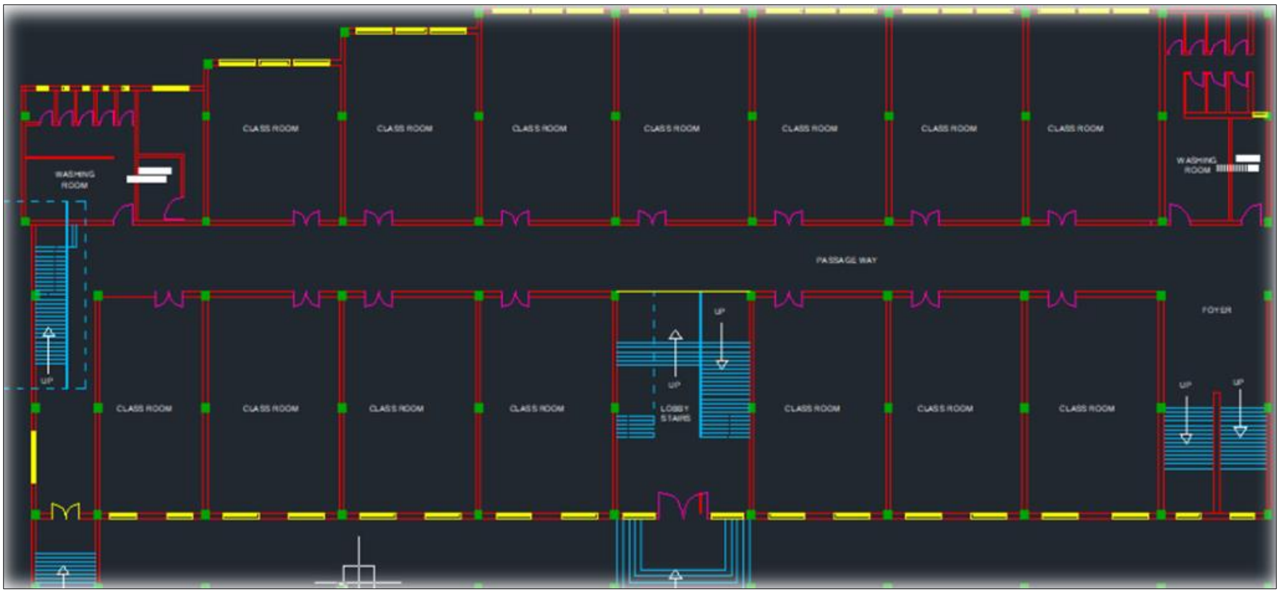

Fig. 3: Ground floor plan

Ground floor plan shows the arrangement of the walls and the rooms, as well as the columns and beams, on the building's main level. The figure correlates observed crack locations with structural features. We compare the ground floor plan with the basement plan and can tell from this if the cracks seen in the basement run up to continue to destabilize the goods above. This level is particularly important to analyze cracks since the cracks are subjected to more wear and tear from human traffic and environmental exposure as well as significant dynamic loads on this floor.

2.8 Data Collection

Data collection focused on cracks present in different parts of the Al-Beruni Block, specifically in the columns, beams, and slabs. A total of 13 cracks were identified across various laboratories within the university, including:

Fluid Mechanics Lab: Cracks 1–5
Highway Lab: Cracks 6–8
Thermodynamics Lab: Cracks 9–11
Power Plant Lab: Cracks 12–13

For each crack, both plastic tell tales and digital image analysis were employed. Tell tales were installed to monitor real-time movement, while high-resolution images were captured periodically and analyzed using ImageJ. The software was calibrated to the real-world scale by setting pixel-to-millimeter ratios, ensuring accurate measurement of crack expansion over time.

2.8.1 Procedure of Setting up a Crack through Image J

- First open the picture of crack on which tell tales are placed.
- Now set the scale and pixel as software does not know about what scale and pixel we want to use.
- Then analyze and set the scale as pixel are already analyzed by drawing the lines.
- Now select triangle tool and select the area we want to analyze and make a duplicate of it.
- Then use the line tool and draw the line on the crack on different points.
- As a result, we will get the lengths of cracks on different points.
- We will also get the angle of crack and the mean length of all cracks.

2.8.2 Data Collection from Fluid Mechanics Lab

The following data was recorded through ImageJ from the cracks on which tell-tales are present in.

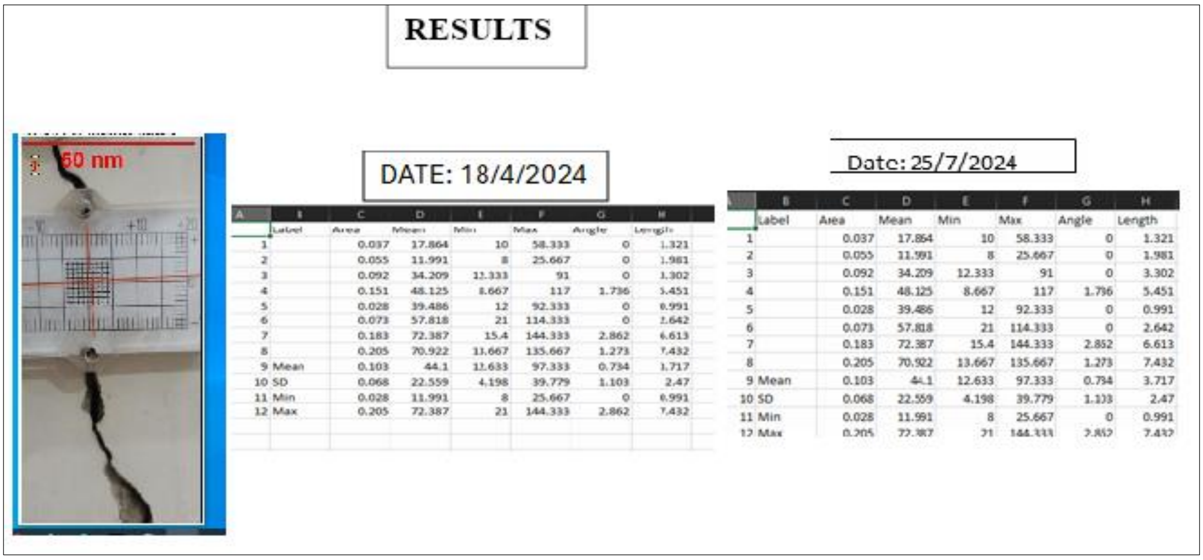

DATE: 18/4/2024

	Label	Area	Mean	Min	Max	Angle	Length
1		0.037	17.864	10	58.333	0	1.321
2		0.055	11.991	8	25.667	0	1.981
3		0.092	34.209	12.333	91	0	3.302
4		0.151	48.125	8.667	117	1.736	5.451
5		0.028	39.486	12	92.333	0	0.991
6		0.073	57.818	21	114.333	0	2.642
7		0.183	72.387	15.4	144.333	2.862	6.613
8		0.205	70.922	13.667	135.667	1.273	7.432
9	Mean	0.103	44.1	12.633	97.333	0.734	3.717
10	SD	0.068	22.559	4.198	39.779	1.103	2.47
11	Min	0.028	11.991	8	25.667	0	0.991
12	Max	0.205	72.387	21	144.333	2.862	7.432

Date: 25/7/2024

	Label	Area	Mean	Min	Max	Angle	Length
1		0.037	17.864	10	58.333	0	1.321
2		0.055	11.991	8	25.667	0	1.981
3		0.092	34.209	12.333	91	0	3.302
4		0.151	48.125	8.667	117	1.736	5.451
5		0.028	39.486	12	92.333	0	0.991
6		0.073	57.818	21	114.333	0	2.642
7		0.183	72.387	15.4	144.333	2.852	6.613
8		0.205	70.922	13.667	135.667	1.273	7.432
9	Mean	0.103	44.1	12.633	97.333	0.734	3.717
10	SD	0.068	22.559	4.198	39.779	1.103	2.47
11	Min	0.028	11.991	8	25.667	0	0.991
12	Max	0.205	72.387	21	144.333	2.852	7.432

Fig. 4: CRACK 1

The movement over time analysis for Crack 1 was significant and showed an active structural distress. Using ImageJ software, along with tell-tale devices, measurements taken revealed the increase in crack width. This implies that Crack 1 is under the effects of continued differential settlement or structural load redistribution. Investigation of this behavior is warranted, since the progression of the crack threatens the integrity of the structure.

DATE: 18/4/2024

	Label	Area	Mean	Min	Max	Angle	Length
1		0.026	32.501	20.76	49.667	15.945	1.04
2		0.011	35.193	22	100.333	0	0.43
3		0.01	98.9	55.803	184	-45	0.40
4		0.025	54.69	17.333	178.333	0	1.00
5		0.045	82.245	15	140.667	0	1.86
6		0.011	60.632	16.667	126	0	0.43
7		0.018	48.075	23.333	87.333	0	0.71
8		0.028	52.449	0	134.333	0	1.14
9		0.045	80.004	34	133	0	1.86
10		0.011	28.195	24.509	34.343	-18.435	0.45
11		0.033	41.484	26.185	55.795	32.005	1.35
12		0.015	68.28	27.157	175.667	-14.036	0.59
13	Mean	0.023	56.887	23.562	116.623	-2.46	0.94
14	SD	0.013	21.98	13.123	51.485	18.508	0.53
15	Min	0.01	28.195	0	34.343	-45	0.40

Date: 25/7/2024

	Label	Area	Mean	Min	Max	Angle	Length
1		0.054	44.082	10.667	108.333	0	1.95
2		0.06	32.72	9	85.333	0	2.16
3		0.071	56.718	13.667	161.667	0	2.60
4		0.018	12.44	11	15	0	0.65
5		0.054	24.717	10	97.333	0	1.95
6		0.036	26.32	12	91.333	0	1.30
7		0.048	54.344	9	155.667	0	1.73
8		0.095	41.354	10.667	109.208	3.576	3.47
9		0.054	71.361	12.667	141.333	-6.34	1.96
10		0.095	44.895	10.062	119	-3.576	3.47
11		0.048	27.769	11	73.375	-7.125	1.74
12	Mean	0.057	39.702	10.884	105.235	-1.224	2.09
13	SD	0.023	17.009	1.444	41.298	3.163	0.84
14	Min	0.018	12.44	9	15	-7.125	0.65

Fig. 5: CRACK 2

Furthermore, Crack 2 measured widening can be attributed to either environmental condition or sub structural shift. Continuous movement was indicated by the use of tell tales, and this section of the building is subject to localized stress. As it is known to progress further, this area should be reinforced in order to prevent its progression in the future and further studies are needed to further isolate the exact cause.

DATE: 18/4/2024

	Label	Area	Mean	Min	Max	Angle	Length
1		0.054	44.082	10.667	108.333	0	1.9
2		0.06	32.72	9	85.333	0	2.1
3		0.071	56.718	13.667	161.667	0	2.6
4		0.018	12.44	11	15	0	0.8
5		0.054	24.717	10	97.333	0	1.9
6		0.036	26.32	12	91.333	0	1.3
7		0.048	54.344	9	155.667	0	1.7
8		0.095	41.354	10.667	109.208	3.576	3.4
9		0.054	71.361	12.667	141.333	-6.34	1.9
10		0.095	44.895	10.062	119	-3.576	3.4
11		0.048	27.769	11	73.375	-7.125	1.3
12	Mean	0.057	39.702	10.884	105.235	-1.224	2.0
13	SD	0.023	17.009	1.444	41.298	3.163	0.8
14	Min	0.018	12.44	9	15	-7.125	0.8
15	Max	0.095	71.361	13.667	161.667	3.576	3.4

Date: 25/7/2024

	Label	Area	Mean	Min	Max	Angle	Length
1		0.028	32.501	20.76	49.667	15.945	1.04
2		0.011	35.193	22	100.333	0	0.43
3		0.01	98.9	55.803	184	-45	0.40
4		0.025	54.69	17.333	178.333	0	1.00
5		0.045	82.245	15	140.667	0	1.86
6		0.011	60.632	16.667	126	0	0.43
7		0.018	48.075	23.333	87.333	0	0.71
8		0.028	52.449	0	134.333	0	1.14
9		0.045	80.004	34	133	0	1.86
10		0.011	28.195	24.509	34.343	-18.435	0.45
11		0.033	41.484	26.185	55.795	32.005	1.33
12		0.015	68.28	27.157	175.667	-14.036	0.59
13	Mean	0.023	56.887	23.562	116.623	-2.46	0.94
14	SD	0.013	21.98	13.123	51.485	18.508	0.53
15	Min	0.01	28.195	0	34.343	-45	0.40
16	Max	0.045	98.9	55.803	184	32.005	[illegible]

Fig. 6: CRACK 3

No movement was observed with Crack 3 suggesting a state of dormancy. Or perhaps it has reached equilibrium and was already there from previous settling. Although the risk of further expansion is now relatively low, the crack should be monitored periodically to maintain its stability in time, in particular under changing load condition.

DATE: 18/4/2024

	Label	Area	Mean	Min	Max	Angle	Length
1		0.093	100.765	90.095	128.667	-81.87	1.115
2		0.05	110.527	91.946	147.333	-56.31	0.569
3		0.087	121.802	66.661	204	18.435	0.997
4		0.031	127.4	74	198	0	0.315
5		0.087	99.672	76	112.797	51.34	1.01
6		0.044	114.429	90	162	0	0.473
7		0.131	110.515	80.947	145	53.13	1.577
8		0.131	92.302	70	110.333	0	1.577
9		0.118	119.281	90.667	141	-6.34	1.428
10	Mean	0.086	110.744	81.146	149.903	-2.402	1.007
11	SD	0.037	11.448	9.858	33.335	44.244	0.474
12	Min	0.031	92.302	66.661	110.333	-81.87	0.315
13	Max	0.131	127.4	91.946	204	53.13	1.577

Date: 25/7/2024

	Label	Area	Mean	Min	Max	Angle	Length
1		0.093	100.765	90.095	128.667	-81.87	1.11
2		0.05	110.527	91.946	147.333	-56.31	0.56
3		0.087	121.802	66.661	204	18.435	0.99
4		0.031	127.4	74	198	0	0.31
5		0.087	99.672	76	112.797	51.34	1.0
6		0.044	114.429	90	162	0	0.47
7		0.131	110.515	80.947	145	53.13	1.57
8		0.131	92.302	70	110.333	0	1.57
9		0.118	119.281	90.667	141	-6.34	1.42
10	Mean	0.086	110.744	81.146	149.903	-2.402	1.00
11	SD	0.037	11.448	9.858	33.335	44.244	0.47
12	Min	0.031	92.302	66.661	110.333	-81.87	0.31
13	Max	0.131	127.4	91.946	204	53.13	1.57

Fig. 7: CRACK 4

The active crack was marked as crack 4, with slight progression. Differential settlement, together with seasonal environmental factors such as temperature, may be the primary cause for this movement. Further deterioration.

DATE: 18/4/2024

	Label	Area	Mean	Min	Max	Angle	Length
1		0.043	46.676	11.667	124.333	0	1.74
2		0.025	96.544	45.333	138.945	11.31	0.98
3		0.019	33.404	10.333	100.333	0	0.77
4		0.029	36.368	12.429	122.667	9.462	1.1
5		0.034	40.708	8	160.667	0	1.35
6		0.038	37.4	8	90	0	1.55
7		0.024	28.276	16.667	79	0	0.9
8		0.029	38.291	10	102.333	9.462	1.1
9		0.026	47.185	11.087	130.667	21.801	1.04
10		0.062	88.317	14.333	131	0	2.52
11	Mean	0.033	49.317	14.785	117.995	5.204	1.33
12	SD	0.012	23.486	11.059	24.75	7.539	0.50
13	Min	0.019	28.276	8	79	0	0.77
14	Max	0.062	96.544	45.333	160.667	21.801	2.52

Date: 25/7/2024

	Label	Area	Mean	Min	Max	Angle	Length
1		0.043	46.676	11.667	124.333	0	1.74
2		0.025	96.544	45.333	138.945	11.31	0.98
3		0.019	33.404	10.333	100.333	0	0.77
4		0.029	36.368	12.429	122.667	9.462	1.1
5		0.034	40.708	8	160.667	0	1.35
6		0.038	37.4	8	90	0	1.55
7		0.024	28.276	16.667	79	0	0.9
8		0.029	38.291	10	102.333	9.462	1.1
9		0.026	47.185	11.087	130.667	21.801	1.04
10		0.062	88.317	14.333	131	0	2.52
11	Mean	0.033	49.317	14.785	117.995	5.204	1.33
12	SD	0.012	23.486	11.059	24.75	7.539	0.50
13	Min	0.019	28.276	8	79	0	0.77
14	Max	0.062	96.544	45.333	160.667	21.801	2.52

Fig. 8: CRACK 5

The progression of Crack 5 was recorded, noting widening during heat cycles. The results suggest thermal expansion and compaction are at play. Bands of thermal insulation and sealing should be applied to affected areas, as far as practical, to minimize effects on temperature on structural stability.

2.8.3 Data Collection from Highway Lab

The following data was recorded through ImageJ from the cracks on which tell-tales are present in highway lab.

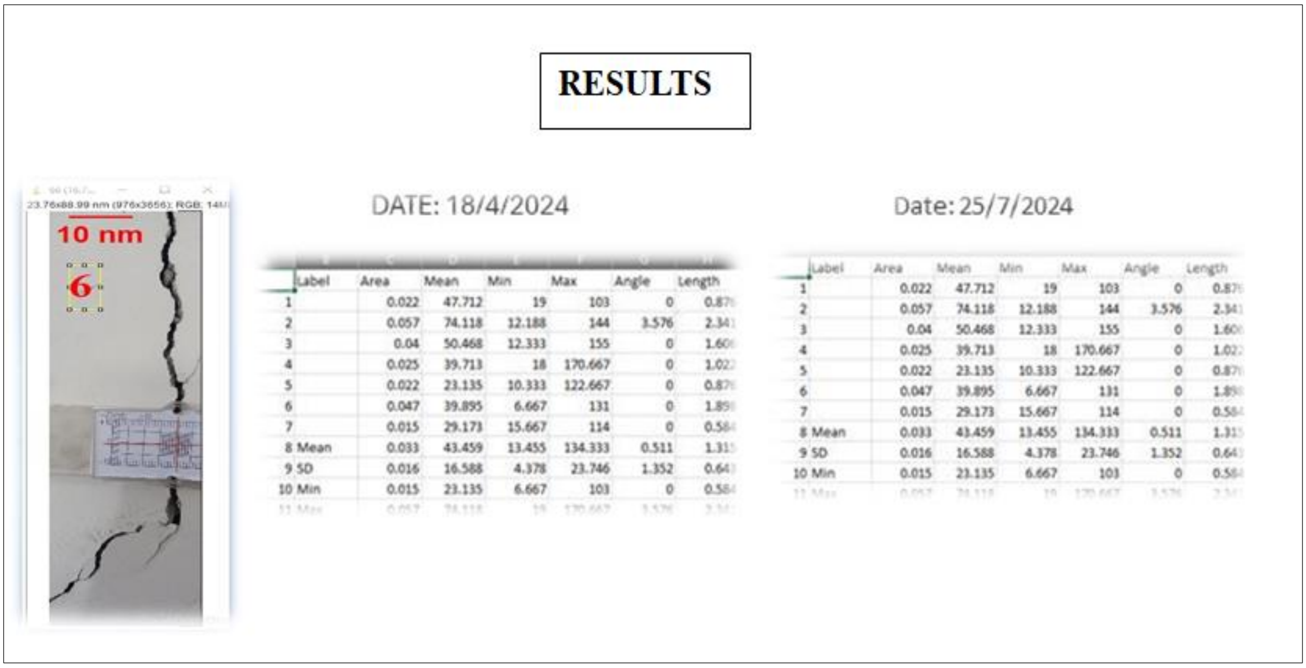

DATE: 18/4/2024

	Label	Area	Mean	Min	Max	Angle	Length
1		0.022	47.712	19	103	0	0.87
2		0.057	74.118	12.188	144	3.576	2.34
3		0.04	50.468	12.333	155	0	1.60
4		0.025	39.713	18	170.667	0	1.02
5		0.022	23.135	10.333	122.667	0	0.87
6		0.047	39.895	6.667	131	0	1.89
7		0.015	29.173	15.667	114	0	0.58
8	Mean	0.033	43.459	13.455	134.333	0.511	1.31
9	SD	0.016	16.588	4.378	23.746	1.352	0.64
10	Min	0.015	23.135	6.667	103	0	0.58
11	Max	0.057	74.118	19	170.667	3.576	2.34

Date: 25/7/2024

	Label	Area	Mean	Min	Max	Angle	Length
1		0.022	47.712	19	103	0	0.87
2		0.057	74.118	12.188	144	3.576	2.34
3		0.04	50.468	12.333	155	0	1.60
4		0.025	39.713	18	170.667	0	1.02
5		0.022	23.135	10.333	122.667	0	0.87
6		0.047	39.895	6.667	131	0	1.89
7		0.015	29.173	15.667	114	0	0.58
8	Mean	0.033	43.459	13.455	134.333	0.511	1.31
9	SD	0.016	16.588	4.378	23.746	1.352	0.64
10	Min	0.015	23.135	6.667	103	0	0.58
11	Max	0.057	74.118	19	170.667	3.576	2.34

Fig. 9: CRACK 6

In the highway laboratory crack 6 was wide and had contributed to the fatigue of material due to repetitive loads and vibration. According to the data it is more likely that dynamic loading will result in structural stress, both of which can be alleviated by material reinforcement or vibration dampening. If this crack is not attended to it may put the structural integrity of the ship at risk.

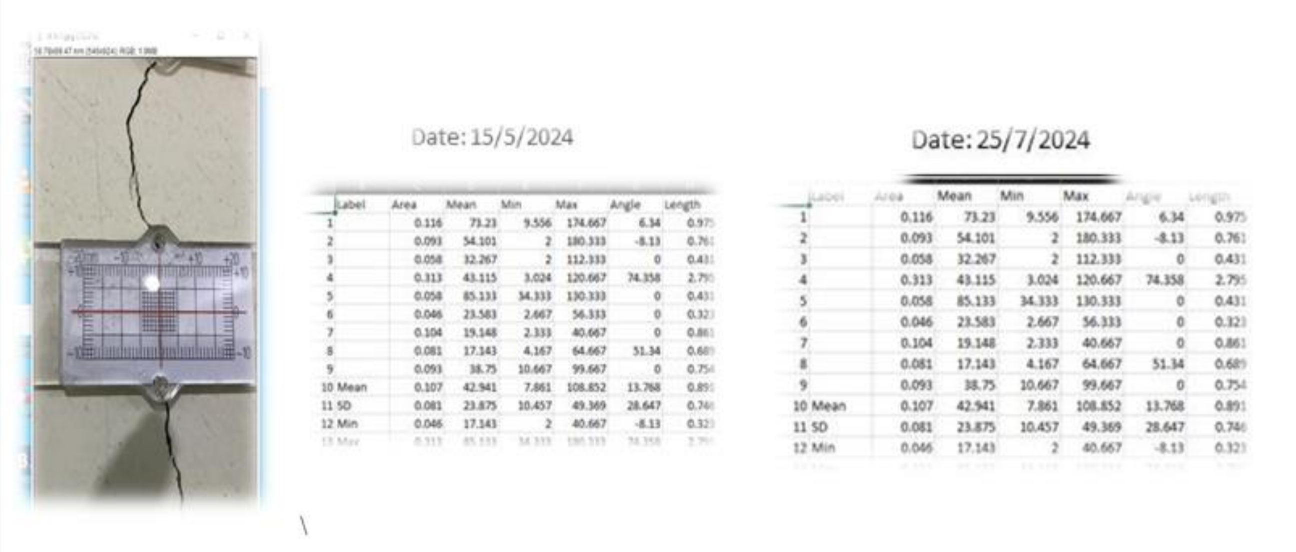

Fig. 10: CRACK 7

The movement shown by Crack 7 was probably due to mechanical stress and material degradation with time. The stress condition behavior of this crack point to the potential flaws in the construction materials or design. Prevention of further structural damage requires immediate reinforcement.

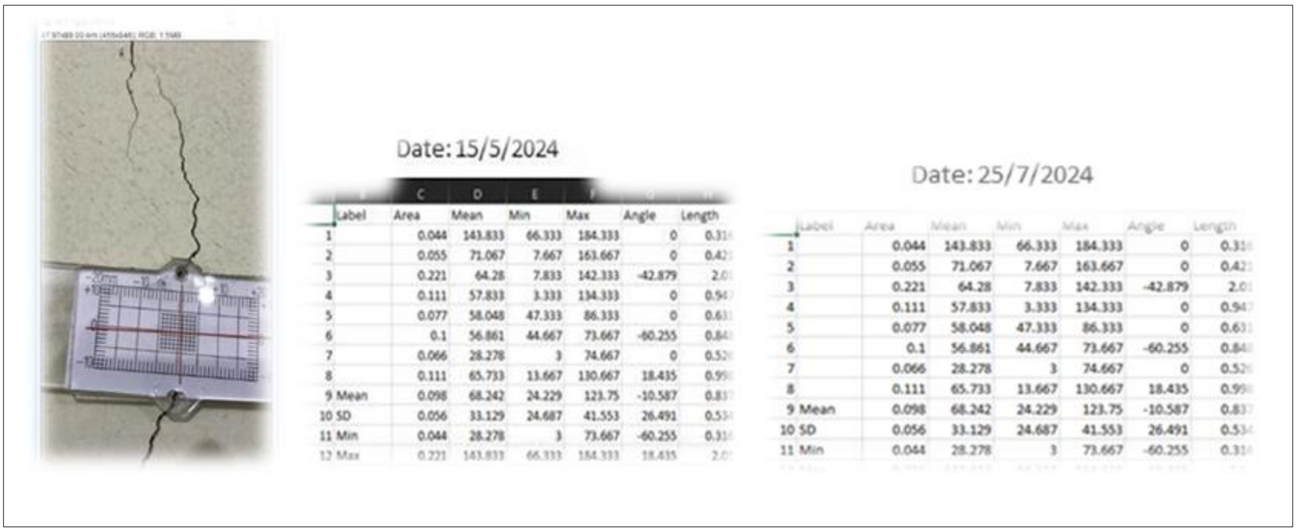

Fig. 11: CRACK 8

It showed only minimal progression, indicating that crack 8 is very dormant. But as with the crack, environmental monitoring is needed to make sure it stays stable. This crack is not an immediate threat; however, this crack should be observed periodically to determine if further movement will occur.

2.8.4Data Collection from Fluid Thermodynamics Lab

The following data was recorded through ImageJ from the crack on which tell-tales that are present in thermodynamics lab.

RESULTS

Date: 15/5/2024

	Label	Area	Mean	Min	Max	Angle	Length
1		0.308	52.94	1.267	155	2.862	2.427
2		0.294	35.217	11.667	75.667	0	2.303
3		0.235	29.667	4.667	103	0	1.818
4		0.279	24.003	2.667	82.167	-3.18	2.185
5		0.558	14.045	1.346	34	-30.7	4.51
6		0.235	33.321	1	157.667	-11.31	1.854
7		0.235	30.917	0.333	137.667	0	1.818
8		0.206	23.938	4.615	91.667	4.399	1.58
9		0.25	28.358	1.917	89	14.036	1.999
10	Mean	0.289	30.267	3.275	102.87	-2.655	2.277
11	SD	0.106	10.576	3.499	40.56	12.458	0.879
12	Min	0.206	14.045	0.333	34	-30.7	1.58
13	Max	0.558	52.94	11.667	157.667	14.036	4.51

Date: 25/7/2024

	Label	Area	Mean	Min	Max	Angle	Length
1		0.308	52.94	1.267	155	2.862	[illegible]
2		0.294	35.217	11.667	75.667	0	[illegible]
3		0.235	29.667	4.667	103	0	[illegible]
4		0.279	24.003	2.667	82.167	-3.18	[illegible]
5		0.558	14.045	1.346	34	-30.7	[illegible]
6		0.235	33.321	1	157.667	-11.31	[illegible]
7		0.235	30.917	0.333	137.667	0	[illegible]
8		0.206	23.938	4.615	91.667	4.399	[illegible]
9		0.25	28.358	1.917	89	14.036	[illegible]
10	Mean	0.289	30.267	3.275	102.87	-2.655	[illegible]
11	SD	0.106	10.576	3.499	40.56	12.458	[illegible]
12	Min	0.206	14.045	0.333	34	-30.7	[illegible]

Fig. 12: CRACK 9

Expansion from crack 9 in the Fluid Thermodynamics Lab was consistent with thermal fluctuations. The crack progresses primarily in response to temperature variations, according to the data. This further damage has to be mitigated through the introduction of thermal control measure such as insulation or expansion joints.

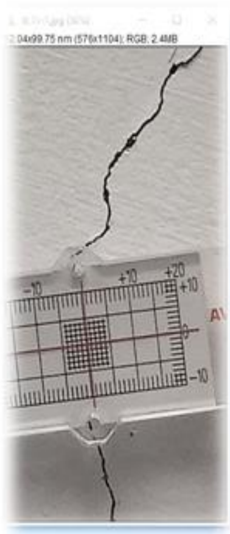

Date: 15/5/2024

	Label	Area	Mean	Min	Max	Angle	Length
1		0.22	57.483	1	208.333	-8.746	2.377
2		0.155	111.491	6.333	213.333	0	1.626
3		0.098	34.687	11.887	103.333	-45	1.022
4		0.131	47.808	9.28	201.667	23.199	1.376
5		0.073	24.111	2.333	44.333	0	0.723
6		0.09	65.939	5.667	148.667	0	0.904
7		0.073	34.491	1.333	125.667	14.036	0.745
8	Mean	0.12	53.716	5.405	149.333	-2.359	1.253
9	SD	0.053	29.282	4.151	63.268	21.594	0.596
10	Min	0.073	24.111	1	44.333	-45	0.723
11	Max	0.22	111.491	11.887	213.333	23.199	2.377

Date: 25/7/2024

	Label	Area	Mean	Min	Max	Angle	Length
1		0.22	57.483	1	208.333	-8.746	2.377
2		0.155	111.491	6.333	213.333	0	1.626
3		0.098	34.687	11.887	103.333	-45	1.022
4		0.131	47.808	9.28	201.667	23.199	1.376
5		0.073	24.111	2.333	44.333	0	0.723
6		0.09	65.939	5.667	148.667	0	0.904
7		0.073	34.491	1.333	125.667	14.036	0.745
	Mean	0.12	53.716	5.405	149.333	-2.359	1.253
	SD	0.053	29.282	4.151	63.268	21.594	0.596
	Min	0.073	24.111	1	44.333	-45	0.723
	Max	0.22	111.491	11.887	213.333	23.199	2.377

Fig. 13: CRACK 10

Similar thermal induced behavior was shown in Crack 10, with a minor but consistent widening. This implies that the development of crack is associated with temperature related stresses. Recommendations for keeping additional expansion limitation include thermal insulation and reinforcement of the material.

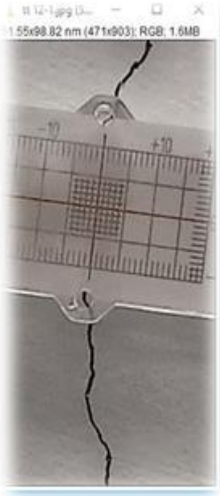

Date: 15/5/2024

	Label	Area	Mean	Min	Max	Angle	Length
1		0.228	46.577	1.667	161.667	-6.34	1.9
2		0.156	17.821	3.667	89.667	0	1.3
3		0.084	64.381	1.333	202.333	0	0.6
4		0.108	55.37	2.333	137.667	0	0.8
5		0.084	40.381	4.667	129.667	0	0.6
6		0.132	41.315	1.667	132.267	11.31	1.1
7		0.084	16.683	2.667	70.333	-18.435	0.6
8	Mean	0.125	40.361	2.571	131.943	-1.924	1.0
9	SD	0.053	17.844	1.213	43.702	8.963	0.4
10	Min	0.084	16.683	1.333	70.333	-18.435	0.6

Date: 25/7/2024

	Label	Area	Mean	Min	Max	Angle	Length
1		0.228	46.577	1.667	161.667	-6.34	1.9
2		0.156	17.821	3.667	89.667	0	1.3
3		0.084	64.381	1.333	202.333	0	0.6
4		0.108	55.37	2.333	137.667	0	0.8
5		0.084	40.381	4.667	129.667	0	0.6
6		0.132	41.315	1.667	132.267	11.31	1.1
7		0.084	16.683	2.667	70.333	-18.435	0.6
8	Mean	0.125	40.361	2.571	131.943	-1.924	1.0
9	SD	0.053	17.844	1.213	43.702	8.963	0.4
10	Min	0.084	16.683	1.333	70.333	-18.435	0.6

Fig. 14: CRACK 11

The observation that Crack 11 was largely stable, showing no significant movement during the observation period, supported the view that the succession following perturbation was limited. This crack is currently inactive but is being monitored because it may resume activity if changes in environmental condition or structural loading occur.

2.8.5Data Collection from Fluid Power Plant Lab

The following data was recorded through ImageJ from the crack on which tell tales are present in power plant lab

RESULTS

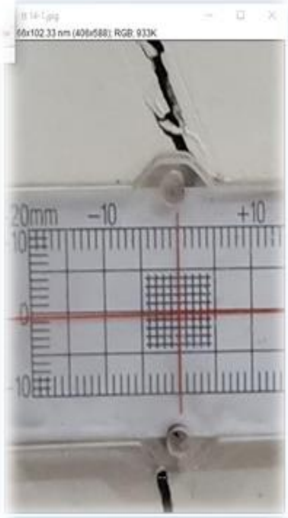

Date: 15/5/2024

	Label	Area	Mean	Min	Max	Angle	Length
1		0.515	14.197	1.688	73	-3.576	2.7
2		0.394	36.179	2.667	122.333	0	2.08
3		0.666	66.805	1.626	184	-14.036	3.58
4		1.06	66.417	1.78	160.902	11.976	5.871
5		1.03	91.418	34	178.667	-15.709	5.78
6		0.515	23.039	1.333	135.333	0	2.78
7		0.424	19.738	3.333	108.333	0	2.26
8	Mean	0.658	45.399	6.632	137.51	-3.049	3.59
9	SD	0.279	29.537	12.088	40.105	9.442	1.59
10	Min	0.394	14.197	1.333	73	-15.709	2.08
11	Max	1.06	91.418	34	184	11.976	5.871

DATE: 25/7/2024

	Label	Area	Mean	Min	Max	Angle	Length
1		0.515	14.197	1.688	73	-3.576	2.7
2		0.394	36.179	2.667	122.333	0	2.08
3		0.666	66.805	1.626	184	-14.036	3.58
4		1.06	66.417	1.78	160.902	11.976	5.871
5		1.03	91.418	34	178.667	-15.709	5.78
6		0.515	23.039	1.333	135.333	0	2.78
7		0.424	19.738	3.333	108.333	0	2.26
8	Mean	0.658	45.399	6.632	137.51	-3.049	3.59
9	SD	0.279	29.537	12.088	40.105	9.442	1.59
10	Min	0.394	14.197	1.333	73	-15.709	2.08
11	Max	1.06	91.418	34	184	11.976	5.871

Fig. 15: CRACK 12

The Fluid Power Plant Lab: crack 12, had seen widening which was probably from a vibration during operating of machines. This area demonstrates that mechanical stresses in the area dictate the need for structural reinforcement or vibration dampening to prevent further damage.

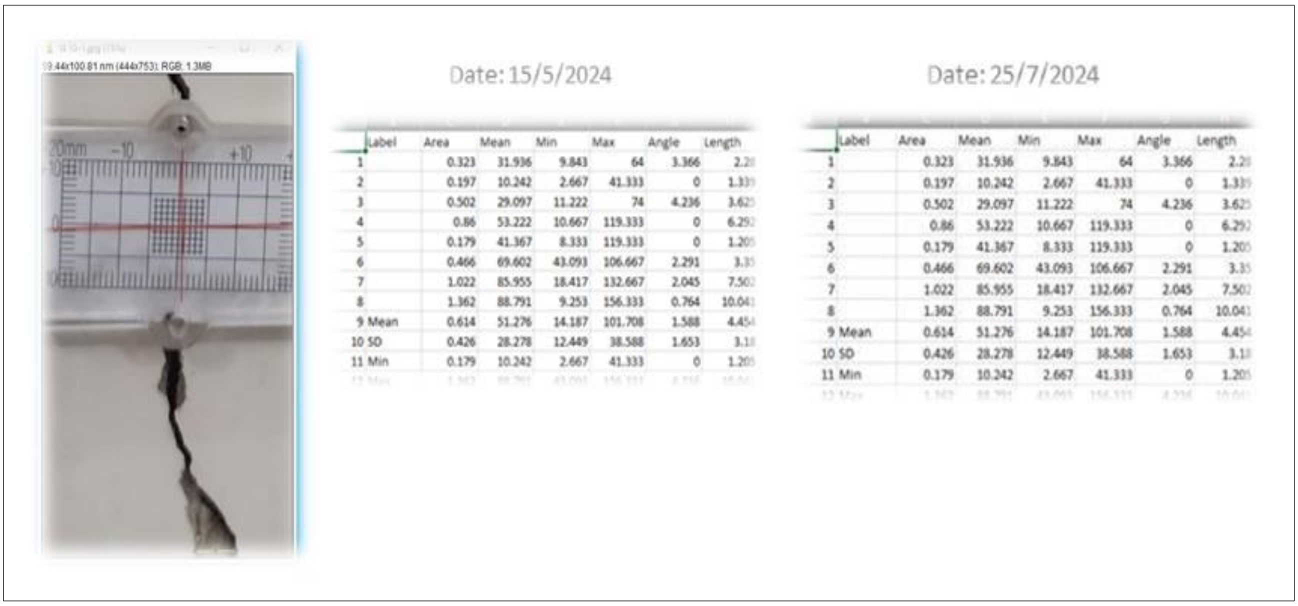

Date: 15/5/2024

	Label	Area	Mean	Min	Max	Angle	Length
1		0.323	31.936	9.843	64	3.366	2.2[illegible]
2		0.197	10.242	2.667	41.333	0	1.33[illegible]
3		0.502	29.097	11.222	74	4.236	3.62[illegible]
4		0.86	53.222	10.667	119.333	0	6.29[illegible]
5		0.179	41.367	8.333	119.333	0	1.20[illegible]
6		0.466	69.602	43.093	106.667	2.291	3.3[illegible]
7		1.022	85.955	18.417	132.667	2.045	7.50[illegible]
8		1.362	88.791	9.253	156.333	0.764	10.04[illegible]
9	Mean	0.614	51.276	14.187	101.708	1.588	4.45[illegible]
10	SD	0.426	28.278	12.449	38.588	1.653	3.1[illegible]
11	Min	0.179	10.242	2.667	41.333	0	1.20[illegible]

Date: 25/7/2024

	Label	Area	Mean	Min	Max	Angle	Length
1		0.323	31.936	9.843	64	3.366	2.2[illegible]
2		0.197	10.242	2.667	41.333	0	1.33[illegible]
3		0.502	29.097	11.222	74	4.236	3.62[illegible]
4		0.86	53.222	10.667	119.333	0	6.29[illegible]
5		0.179	41.367	8.333	119.333	0	1.20[illegible]
6		0.466	69.602	43.093	106.667	2.291	3.3[illegible]
7		1.022	85.955	18.417	132.667	2.045	7.50[illegible]
8		1.362	88.791	9.253	156.333	0.764	10.04[illegible]
9	Mean	0.614	51.276	14.187	101.708	1.588	4.45[illegible]
10	SD	0.426	28.278	12.449	38.588	1.653	3.1[illegible]
11	Min	0.179	10.242	2.667	41.333	0	1.20[illegible]

Fig. 16: CRACK 13

Vibrations and pressure changes in fluid systems of the lab caused noticeable progress in Crack 13. It is apparent from this data that this part of the structure is under significant stress and corrective action must be taken now. There should be vibration isolation systems as well as reinforcement.

Cracks found on many different sections of the building are symptoms of structural stresses due to environmental factors, material fatigue and mechanical vibrations. ImageJ analysis and tell tales confirm the need for targeted intervention, i.e. reinforcement, thermal insulation, vibration dampening, to prevent further structural degradation. The Al Beruni block needs to be monitored continuously to ensure the safety and longevity of the block.

2.9 Analysis of Displacement-Time Graphs

Displacement-time graphs show how the displacement changes with time. A horizontal line on a displacement-time graph shows that the crack is stationary (not moving because the displacement does not change) A sloping line on a displacement-time graph shows that the crack is expanding. Following are the graphs of the tell tales installed that noticed changes;

The x-axis shows the time in years while the y-axis shows the displacement in mm. Following are the graphs of cracks that expanded with time:

Fig. 17: Displacement time graph

This graph shows how the displacement in mm per time (in years) changes for a specific crack or group of cracks in a building. The graph shows us the displacement, to be the widening of the crack, on the y axis, and the time on the x axis.

A horizontal line on the graph indicates that the crack is stable and has not widened during the time that was observed. Such that the crack is not presently experiencing a progression, which could indicate that the structural stability in that area is also being maintained.

This is shown by a sloping line, which means that the crack is growing with time. The slope of the line in Graph is gradual, indicating that the crack is opening at a fairly slow, but also fairly constant rate. That may suggest that you should monitor it regularly, but it doesn't mean it's an immediate threat.

3. RESULTS AND DISCUSSION

3.1 Performance of Plastic Tell Tales

Plastic tell tales proved to be an effective tool for initial crack monitoring, offering a visual representation of crack movement. While some cracks remained stable throughout the monitoring period, others displayed noticeable displacement, indicating ongoing structural adjustments. The tell tales were especially useful for detecting shear and normal movements in cracks located in the columns and beams.

3.2 Comparative Analysis

The dual approach of using plastic tell tales alongside ImageJ image analysis proved to be highly complementary. While plastic tell tales provided immediate visual feedback, ImageJ offered a more precise and quantitative analysis of crack progression. This hybrid method addressed the limitations of each technique when used in isolation, resulting in a more complete understanding of the structural health of the Al-Beruni Block.

4. CONCLUSION

- Our research was based on crack monitoring which we carried out since Dec 2023 in result we can say that regular monitoring of the present cracks is required as new cracks can be seen in the building.
- A crack that was monitored did not show any changes during our research.
- The changes do not occur because Al-Beruni block was made in 2015 and we know that after some 3 ,4 years' period of time no more changes can be happened in cracks due to settlement of the building.

5. RECOMMENDATIONS

Continued Monitoring:

Ongoing monitoring of the identified cracks is recommended, especially for those showing signs of movement. New cracks should be mapped and monitored as soon as they are detected.

Expansion to other Structures:

This hybrid monitoring approach could be adapted for use in other civil structures, such as bridges, tunnels, and high-rise buildings, where continuous monitoring is essential for safety and maintenance.

Seismic Activity Consideration:

Given the geographical location of the Al-Beruni Block, future studies should explore the impact of seismic events on crack propagation, using the dual monitoring approach to capture real-time changes during and after seismic activity.

6. Acknowledgments

The authors express their gratitude to Sarhad University for providing access to the Al-Beruni Block and for their support in data collection. Special thanks are extended to the laboratory staff for their assistance throughout the research process.

REFERENCES

1. Ozer, E., & Feng, M. Q. (2020). Structural health monitoring. In *Start-up creation* (pp. 345-367). Woodhead Publishing.
2. Smith, B. J., Kurama, Y. C., & McGinnis, M. J. (2011). Design and measured behavior of a hybrid precast concrete wall specimen for seismic regions. *Journal of Structural Engineering*, *137*(10), 1052-1062.
3. Li, W., Xu, C., Ho, S. C. M., Wang, B., & Song, G. (2017). Monitoring concrete deterioration due to reinforcement corrosion by integrating acoustic emission and FBG strain measurements. *Sensors*, *17*(3), 657.
4. Hamdan, A., & Mustapha, F. (2019). Structural Health Monitoring of Biocomposites, Fibre-Reinforced Composites, and Hybrid Composites. *Structural Health Monitoring*.
5. Ozer, E., & Feng, M. Q. (2020). Advances in Structural Health Monitoring through Smart and Mobile Sensor Systems. Start-Up Creation (Second Edition).
6. Krakhmal'ny, T. A., Evtushenko, S. I., & Krakhmal'naya, M. P. (2019). Remote Monitoring System for Small Reinforced Concrete Bridges.
7. Van Steen, C., & Verstrynge, E. (2021). Degradation monitoring in reinforced concrete with 3D localization of rebar corrosion and related concrete cracking. *Applied Sciences*, *11*(15), 6772.
8. Charbonnel, P. É. (2021). Fuzzy-driven strategy for fully automated modal analysis: Application to the SMART2013 shaking-table test campaign. *Mechanical Systems and Signal Processing*, *152*, 107388.
9. Russotto, S., Di Matteo, A., & Pirrotta, A. (2022). An innovative structural dynamic identification procedure combining time domain OMA technique and GA. *Buildings*, *12*(7), 963.
10. Bogusz, P., Krasoń, W., & Pazur, K. (2024). Application of Digital Image Correlation for Strain Mapping of Structural Elements and Materials. *Materials*, *17*(11), 2577.
11. Di. Matteo, A., Masnata, C., Russotto, S., Bilello, C., & Pirrotta, A. (2021). A novel identification procedure from ambient vibration data. *Meccanica*, *56*, 797-812.
12. Barone, G., Marino, F., & Pirrotta, A. (2008). Low stiffness variation in structural systems: identification and localization. *Structural Control*

and Health Monitoring: The Official Journal of the International Association for Structural Control and Monitoring and of the European Association for the Control of Structures, *15*(3), 450-470.
13. Romano, P., Brito, P. S., & Rodrigues, L. (2013). Monitoring of the degradation of concrete structures in environments containing chloride ions. *Construction and Building Materials*, *47*, 827-832.
14. Coppola, L., Beretta, S., Bignozzi, M. C., Bolzoni, F., Brenna, A., Cabrini, M., ... & Todaro, F. (2022). The improvement of durability of reinforced concretes for sustainable structures: A review on different approaches. *Materials*, *15*(8), 2728.
15. Ekolu, S. O. (2016). A review on effects of curing, sheltering, and CO2 concentration upon natural carbonation of concrete. *Construction and Building Materials*, *127*, 306-320.
16. Malekjafarian, A., McGetrick, P. J., & OBrien, E. J. (2015). A review of indirect bridge monitoring using passing vehicles. *Shock and vibration*, *2015*(1), 286139.
17. Tronci, E. M., De Angelis, M., Betti, R., & Altomare, V. (2022). Multi-stage semi-automated methodology for modal parameters estimation adopting parametric system identification algorithms. *Mechanical Systems and Signal Processing*, *165*, 108317.
18. Alessi, A., Carcara, F., Ceraulo, M., Cina', G., De Luca, S., Giannici, F., Giarrusso, R., Inguanta, R., La Mantia, F. P., & Mistretta, M. C. (2015). System and method for detecting and monitoring chlorine ion concentration and ph in concrete structures. IT Patent Application No. 1423532; UAE Patent Application No. P6000163/2016 EU Patent application No. 15716866.7-1020.
19. Di Matteo, A., Fiandaca, D., & Pirrotta, A. (2022). Smartphone-based bridge monitoring through vehicle–bridge interaction: analysis and experimental assessment. *Journal of Civil Structural Health Monitoring*, *12*(6), 1329-1342.
20. Sani, M. S. M., Rahman, M. M., Noor, M. M., Kadirgama, K., & Izham, M. H. N. (2011, February). Identification of dynamics modal parameter for car chassis. In *IOP Conference Series: Materials Science and Engineering* (Vol. 17, No. 1, p. 012038). IOP Publishing.
21. Shi, K., Mo, X. Q., Xu, H., Wang, Z. L., Hu, X. S., & Yang, Y. B. (2022). Furthering extraction of torsional–flexural frequencies for thin-wall beams from the rocking motion of a two-wheel test vehicle. *Thin-Walled Structures*, *175*, 109224.
22. Bard, A. J., Faulkner, L. R., & White, H. S. (2022). *Electrochemical methods: fundamentals and applications*. John Wiley & Sons.
23. Figueira, R. B. (2017). Electrochemical sensors for monitoring the corrosion conditions of reinforced concrete structures: A review. *Applied Sciences*, *7*(11), 1157.
24. Peters, W. H., & Ranson, W. F. (1982). Digital imaging techniques in experimental stress analysis. *Optical engineering*, *21*(3), 427-431.
25. Bolhassani, M., Rajaram, S., Hamid, A. A., Kontsos, A., & Bartoli, I. (2016). Damage Detection of Concrete Masonry Structures by Enhancing Deformation Measurement Using DIC; Proceedings of the Nondestructive Characterization and Monitoring of Advanced Materials, Aerospace, and Civil Infrastructure 2016; Las Vegas, NV, USA. 980411.
26. Kumar, S. L., Aravind, H. B., & Hossiney, N. (2019). Digital image correlation (DIC) for measuring strain in brick masonry specimen using Ncorr open source 2D MATLAB program. *Results in Engineering*, *4*, 100061.
27. Nghiem, H. L., Al Heib, M., & Emeriault, F. (2015). Method based on digital image correlation for damage assessment in masonry structures. *Engineering Structures*, *86*, 1-15.
28. Torres, B., Varona, F. B., Baeza, F. J., Bru, D., & Ivorra, S. (2020). Study on retrofitted masonry elements under shear using digital image correlation. *Sensors*, *20*(7), 2122.
29. Ramos, T., Furtado, A., Eslami, S., Alves, S., Rodrigues, H., Arêde, A., ... & Moreira, P. M. G. P. (2015). 2D and 3D digital image correlation in civil engineering–measurements in a masonry wall. *Procedia Engineering*, *114*, 215-222.
30. Furtado, A., Ramos, T., Rodrigues, H., Arêde, A., Varum, H., & Tavares, P. (2015). In-plane response of masonry infill walls: experimental study using digital image correlation. *Procedia Engineering*, *114*, 870-876.
31. Mojsilović, N., & Salmanpour, A. H. (2016). Masonry walls subjected to in-plane cyclic loading: application of digital image correlation for deformation field measurement. *International Journal of Masonry Research and Innovation*, *1*(2), 165-187.
32. Salmanpour, A., & Mojsilovic, N. (2013, December). Application of digital image correlation for strain measurements of large masonry walls. In *Proceedings of the 5th Asia Pacific congress on computational mechanics* (p. 1128).
33. Hossain, M. A., Totoev, Y. Z., & Masia, M. J. (2021). Application of digital image correlation (DIC) technique for semi interlocking masonry (SIM) panels under large cyclic in-plane shear displacement. *Experimental Techniques*, *45*, 509-530.
34. Ghorbani, R., Matta, F., & Sutton, M. A. (2015). Full-field deformation measurement and crack mapping on confined masonry walls using digital image correlation. *Experimental Mechanics*, *55*, 227-243.
35. Shih, M. H., & Sung, W. P. (2014). Developing dynamic digital image correlation technique to monitor structural damage of old buildings under

external excitation. *Shock and vibration*, *2014*(1), 954840.
36. Chang, C. Y., & Huang, C. W. (2020). Non-contact measurement of inter-story drift in three-layer RC structure under seismic vibration using digital image correlation. *Mechanical Systems and Signal Processing*, *136*, 106500.
37. Beberniss, T. J., & Ehrhardt, D. A. (2017). High-speed 3D digital image correlation vibration measurement: Recent advancements and noted limitations. *Mechanical Systems and Signal Processing*, *86*, 35-48.
38. Zona, A. (2021). Vision-Based Vibration Monitoring of Structures and Infrastructures: An Overview of Recent Applications. Infrastructures, *6*(4). doi: 10.3390/infrastructures6010004.
39. Helfrick, M. N., Niezrecki, C., Avitabile, P., & Schmidt, T. (2011). 3D digital image correlation methods for full-field vibration measurement. *Mechanical systems and signal processing*, *25*(3), 917-927.
40. Ngeljaratan, L., & Moustafa, M. A. (2017, September). Digital Image Correlation for dynamic shake table test measurements. In *7th International Conference on Advances in Experimental Structural Engineering (7AESE), September* (pp. 6-8).
41. Kalaitzakis, M., Kattil, S. R., Vitzilaios, N., Rizos, D., & Sutton, M. (2019). Dynamic Structural Health Monitoring Using a DIC-Enabled Drone; Proceedings of the 2019 International Conference on Unmanned Aircraft Systems, ICUAS; Atlanta, GA, USA. 11–14, 321–327.
42. Felipe-Sesé, L., Molina-Viedma, Á., López-Alba, E., & Díaz, F. (2018, June). Dynamic displacements measurement employing fringe projection and digital image correlation. In *Proceedings* (Vol. 2, No. 8, p. 458). MDPI.
43. Shih, M. H., Sung, W. P., & Tsai, F. J. (2011). Analysis accuracy of digital image correlation technique to monitor natural frequency response of building under dynamic excitation. *Applied Mechanics and Materials*, *71*, 3904-3908.
44. Tian, L., Zhang, X., & Pan, B. (2021). Cost-Effective and Ultraportable Smartphone-Based Vision System for Structural Deflection Monitoring. *Journal of Sensors*, *2021*(1), 8843857.
45. Wang, N., Ri, K., Liu, H., & Zhao, X. (2018). Notice of removal: structural displacement monitoring using smartphone camera and digital image correlation. *IEEE Sensors Journal*, *18*(11), 4664-4672.
46. Yu, L., Tao, R., & Lubineau, G. (2019). Accurate 3D shape, displacement and deformation measurement using a smartphone. *Sensors*, *19*(3), 719.
47. Mousa, M. A., & Yussof, M. M. (2021). A simple two-dimensional digital image correlation model for out of plane displacement using smartphone camera. *J. Eng. Sci. Technol*, *16*, 10-17.
48. Yu, L., Bekdullayev, N., & Lubineau, G. (2021). Smartphone-based single-camera stereo-DIC system: thermal error analysis and design recommendations. *IEEE Sensors Journal*, *21*(7), 9567-9576.
49. Yu, L., & Lubineau, G. (2021). A smartphone camera and built-in gyroscope based application for non-contact yet accurate off-axis structural displacement measurements. *Measurement*, *167*, 108449.
50. Yu, L., & Pan, B. (2014). In-plane displacement and strain measurements using a camera phone and digital image correlation. *Optical Engineering*, *53*(5), 054107-054107.
51. Alam, S. Y., Saliba, J., & Loukili, A. (2014). Fracture examination in concrete through combined digital image correlation and acoustic emission techniques. *Construction and Building Materials*, *69*, 232-242.
52. Omondi, B., Aggelis, D. G., Sol, H., & Sitters, C. (2016). Improved crack monitoring in structural concrete by combined acoustic emission and digital image correlation techniques. *Structural Health Monitoring*, *15*(3), 359-378.
53. Hertzberg, R. W., Vinci, R. P., & Hertzberg, J. L. (2020). *Deformation and fracture mechanics of engineering materials*. John Wiley & Sons.
54. Kendall, K. (2020). *Crack control: using fracture theory to create tough new materials*. Elsevier.
55. Parente, L., Falvo, E., Castagnetti, C., Grassi, F., Mancini, F., Rossi, P., & Capra, A. (2022). Image-based monitoring of cracks: Effectiveness analysis of an open-source machine learning-assisted procedure. *Journal of Imaging*, *8*(2), 22.
56. Sreedhara, S., Sorensen, T. J., Poursaee, A., & Ross, B. E. (2023). Practical application of digital image processing in measuring concrete crack widths in field studies. *Practice Periodical on Structural Design and Construction*, *28*(1), 05022006.
57. Harirchian, E., Lahmer, T., Buddhiraju, S., Mohammad, K., & Mosavi, A. (2020). Earthquake safety assessment of buildings through rapid visual screening. *Buildings*, *10*(3), 51.
58. Yadollahi, M., Adnan, A., & Zin, R. M. (2012). Seismic vulnerability functional method for rapid visual screening of existing buildings. *Archives of Civil Engineering*, 363-377.
59. Rajarathnam, S., & Santhakumar, A. R. (2015). Assessment of seismic building vulnerability based on rapid visual screening technique aided by aerial photographs on a GIS platform. *Natural Hazards*, *78*, 779-802.
60. Raoufy, A. A., Kheyroddin, A., & Naderpour, H. (2024). Comparative study of rapid visual screening methods in determining the seismic vulnerability of existing reinforced concrete hospital buildings. *Iranian Journal of Science and Technology, Transactions of Civil Engineering*, *48*(4), 2263-2277.